International Journal of Biological Macromolecules 103 (2017) 525–532

Contents lists available at ScienceDirect

International Journal of Biological Macromolecules

journal homepage: www.elsevier.com/locate/ijbiomac

Molecular cloning and structural modelling of gamma-phospholipase A_2 inhibitors from *Bothrops atrox* and *Micrurus lemniscatus* snakes

Carina G. Picelli[a], Rafael J. Borges[b], Carlos A.H. Fernandes[b], Fabio M. Matioli[b], Carla F.C. Fernandes[a], Juliana C. Sobrinho[a], Rudson J. Holanda[a], Luiz S. Ozaki[a,c,d], Anderson M. Kayano[a], Leonardo A. Calderon[a], Marcos R.M. Fontes[b], Rodrigo G. Stábeli[a], Andreimar M. Soares[a,e,*]

[a] *Centro de Estudos de Biomoléculas Aplicadas a Saúde, CEBio, Fundação Oswaldo Cruz, FIOCRUZ, Fiocruz Rondônia and Departamento de Medicina, Universidade Federal de Rondônia, UNIR, 76812-245 Porto Velho, RO, Brazil*
[b] *Departamento de Física e Biofísica, Instituto de Biociências, Universidade Estadual Paulista, UNESP, Botucatu, SP, Brazil*
[c] *Center for the Study of Biological Complexity, Life Sciences, Virginia Commonwealth University, 23284, Richmond, USA*
[d] *PVE-CNPq, Brazil*
[e] *Centro Universitário São Lucas, UNISL, Porto Velho, RO, Brazil*

ARTICLE INFO

Article history:
Received 30 January 2017
Received in revised form 3 May 2017
Accepted 15 May 2017
Available online 18 May 2017

Keywords:
Snakes
Bothrops atrox
Micrurus lemniscatus
Inhibitors of phospholipases A_2
Gamma type phospholipase A_2 inhibitors

ABSTRACT

Phospholipases A_2 inhibitors (PLIs) produced by venomous and non-venomous snakes play essential role in this resistance. These endogenous inhibitors may be classified by their fold in PLIα, PLIβ and PLIγ. Phospholipases A_2 (PLA_2s) develop myonecrosis in snake envenomation, a consequence that is not efficiently neutralized by antivenom treatment. This work aimed to identify and characterize two PLIs from Amazonian snake species, *Bothrops atrox* and *Micrurus lemniscatus*. Liver tissues RNA of specimens from each species were isolated and amplified by RT-PCR using PCR primers based on known PLIγ gene sequences, followed by cloning and sequencing of amplified fragments. Sequence similarity studies showed elevated identity with inhibitor PLIγ gene sequences from other snake species. Molecular models of translated inhibitors' gene sequences resemble canonical three finger fold from PLIγ and support the hypothesis that the decapeptide (residues 107–116) may be responsible for PLA_2 inhibition. Structural studies and action mechanism of these PLIs may provide necessary information to evaluate their potential as antivenom or as complement of the current ophidian accident treatment.

1. Introduction

Snake venom cause physiological disorder in their prey or bitten victims. The disturbances are mainly related to the action of toxins that possess affinity to receptors or ion channels and of enzymes with catalytic activity, which promote homeostatic deviation of the central and peripheral nervous systems, and cardiovascular, neuromotor, and blood coagulation systems. Furthermore, tissue necrosis around the bite, mainly common in *Bothrops* accidents, may result in permanent sequelae [1,2].

An important part of the effects described above is due to the action of phospholipases A_2 (PLA_2s), which are a superfamily of enzymes that specifically catalyze the hydrolysis of the 2-acyl ester bond of glycero-phospholipids in cell membranes, resulting in lysophospholipids and fatty acids such as arachidonic acid. These metabolites act primarily as precursors of inflammatory mediators (eicosanoids), which are all important in intracellular signaling pathways such as neuronal transmission, mitogenesis, smooth muscle contraction, and platelet activation [3,4]. Because of their importance in inflammatory events, this family of proteins is also well studied in autoimmune and inflammatory diseases.

PLA_2s and other snake venom toxins can be inhibited by different molecules that vary in nature, including synthetic or natural chemical agents of animal and plant origin. For example, synthetic low molecular weight heparin, *p*-bromophenacyl bromide, tetracycline, mono/polyclonal antibodies, and natural flavonoids and alkaloids extracted from plants and molecules stemming from marine organisms, are inhibitors of PLA_2 from snake venoms [5].

* Corresponding author at: Centro de Estudos de Biomoléculas Aplicadas a Saúde, CEBio, Fundação Oswaldo Cruz, FIOCRUZ, Fiocruz Rondônia and Departamento de Medicina, Universidade Federal de Rondônia, UNIR, 76812-245 Porto Velho, RO, Brazil.
E-mail address: andreimar.soares@fiocruz.br (A.M. Soares).

http://dx.doi.org/10.1016/j.ijbiomac.2017.05.076
0141-8130/

Molecular structures with inhibitory activities of phospholipase A_2 and metalloproteinase are also known to be found in snakes. These molecules are related to the self-envenoming prevention mechanism [6]. Besides snakes, other animals, mammals, fish and some invertebrates have been studied for natural resistance against snake venoms [7], fungi and bacteria [8].

PLA_2 inhibitors (PLIs) isolated from snake blood may present differences among different snake species PLIs [9]. These molecules are oligomeric, globular, acidic glycoproteins with molecular mass between 75 and 180 kDa. The mechanism of action of secreted PLA_2 inhibitors is through the formation of a soluble complex between the inhibitor and the target enzyme [10]. These inhibitors are classified into three groups, α, β and γ, based on their structural characteristics and may be present in a single snake, whether poisonous or not [11]. Inhibitors from the three groups have been isolated from diverse snake species and families [10,12].

The PLIγs possess the highest inhibitory action among the three groups [13]. They have inhibitory activities on acidic and basic group II as well as on those of group III PLA_2s [14] and are acidic glycoproteins oligomeric, with molecular weights of each monomer between 20 and 31 kDa. The PLIγs have been classified into two subgroups, PLIγ I and II, according to their amino acid sequence, biochemical characteristics and inhibition profile. Members of the PLIγ I subgroup have a heteromeric composition and two subunits (A and B) with less than 33% identity to each other and inhibit groups I, II, and III PLA_2s. Members of the PLIγ II subgroup preferentially inhibits those PLA_2s of group II and are constituted of a single subunit [7,13,15,16]. However, recently the possibility of a second subunit in a PLIγ II from *Crotalus durissus terrificus* has been raised [17].

PLIs are interesting candidates for designing drugs or even as a tool in envenoming treatment, since they inhibit PLA_2 activity and consequently many of the important symptoms of snakebite accidents [13,18]. Furthermore, the study of PLA_2 inhibitors is a critical area of research because of the pharmacological potential of these components in the treatment of inflammation and as a tool to investigate the role of PLA_2s in physiological functions of cell death and injury [19]. In recent years, synthetic derived peptides from PLIγs were showed to have therapeutic potential in PLA_2-related diseases and as antivenom-like bioactive molecules for snake venom neutralization [20,21].

In this study, we performed molecular cloning of PLIγs of the Amazonian occurring snake species, *Bothrops atrox* and *Micrurus lemninscatus*, and build *in silico* models of their structures.

2. Material and methods

2.1. Ethical compliance

This study was approved by the Council of Management of Genetic Patrimony (Conselho de Gestão do Patrimônio Genético) by reviews from CNPq number 010627/2011 and from IBAMA number 27131-1. Snakes specimens required for this study were donated by the wildlife rescue team of the Santo Antônio Hydroelectric Plant project.

2.2. Extraction of RNA

RNA-later® solution (Thermo Fisher Scientific) were added to the dissected liver tissues from the snake specimens and stored in liquid nitrogen at the Oswaldo Cruz Foundation – FIOCRUZ-Rondônia facilities until use. RNA was isolated from 200 mg of frozen liver tissue homogenized in liquid nitrogen using the TRIzol® Plus RNA Purification Kit (Thermo Fisher Scientific), according to the manufacturer's protocols. The purified RNA samples were stored at −80 °C until use.

Table 1
Oligonucleotide primers sequences used for the amplification of *B. atrox*.

PLI (ATG) A – SENSE	5′-ATGAAATCYCTACACACCATCTGCC-3′
PLI (ATG) B – SENSE	5′ATGAAATCYCTACAGATCATCTGTCTTC-3′
PLI (STOP) A – ANTISENSE	5′-ATCAGAGGCTTGCCAATCTGATG-3′
PLI (STOP) B – ANTISENSE	5′-TTATTGTTTTTCAACTTGGATGGC-3′
PLI (STOP) C – ANTISENSE	5′-GGTGACGGAATTATTCRGAAGGTG-3′

2.3. Cloning of the PLA_2 inhibitor genes and sequencing

Oligonucleotide primers (Table 1) for the polymerase chain reaction (PCR) were designed based on known sequences of PLA_2 genes, corresponding to γ type inhibitors and deposited at NCBI (The National Center for Biotechnology Information) GenBank (AB462512, AF211168, AF211166, AF211165, AF211163, AJ249829, AB021425, AB559509, EU155177, EU155169 e AB003472). First stranded cDNA was synthesized from the purified RNAs of the snake specimens liver tissues using the Super Script® III First-strand Synthesis System (Thermo Fisher Scientific) and the kit's oligo(dT) primer. The PLI genes were subsequently amplified using the "pool" of PLIγ designed primers (Table 1) at a final concentration of 0.2 μM, in a volume of containing 5 μL of the first stranded cDNA reaction mixture, 200 μM dNTPs and one unit of HotMaster™Taq DNA polymerase (5 Prime). PCR conditions were: 95 °C for 3 min and 30 cycles at 95 °C for 30 s, 55 °C for 30 s and 70 °C for one minute.

The amplified fragments were cloned into pGEM®-T Easy Vector (Promega Co, Madison, WI, USA). The cloned inserts were purified by colony PCR using the vector primers T7 and SP6 and the amplified fragments sent for sequencing. Sequencing was performed in an ABI Prism® 377 automatic sequencer (Thermo Fisher Scientific)at the company Genomic – Engenharia Molecular in São Paulo, SP, Brazil.

2.4. Alignment and phylogenetic analysis

Different PLIγ were obtained from NCBI GenBank database using BLASTP algorithm [22] and BLOSUM62 substitution matrix, with *B. atrox* PLI sequence as query. The minimum e-value presented by the selected sequences was 1e-^{74}. Multiple sequence alignment was executed using the online program Muscle [23] and phylogenetic tree was build based on the Bayesian method Monte Carlo-Markov chain (MCMC) using the program MrBayes 3.2.6 [24]. Two concurrent MCMC runs of 500,000 generations were performed using four progressively heated chains with a heating parameter of 0.2, tree sampling every 100 generations and a burn-in setting of 250 trees. After, the phylogenetic tree was visualized using Mesquite v. 3.04 program [25].

2.5. Structural modelling and comparison

The deduced PLI amino acid sequences excluding peptide signal were used to generate structural models for both PLIs using Phyre^2 [26] based on Domains II and III of the models of Urokinase plasminogen activator surface receptor (uPAR) from *Mus musculus* (PDB id/chain: 3LAQ/V) [27] and from *Homo sapiens* (PDB id/chain: 1YWH/A) [28]. Since identity difference among isoforms were less than 1%, only one sequence of each snake PLIs were modeled: *B. atrox* (At.PLI2) and *M. lemniscatus* models (mi.PLI1). More than 94% of residues were modeled with confidence higher than 90% based on template homologous proteins (100% chance). The other 10% of the residues are located in C-terminal region, last 9 and 7 residues from *B. atrox* and *M. lemniscatus* models, respectively, and were modeled by *ab initio*.

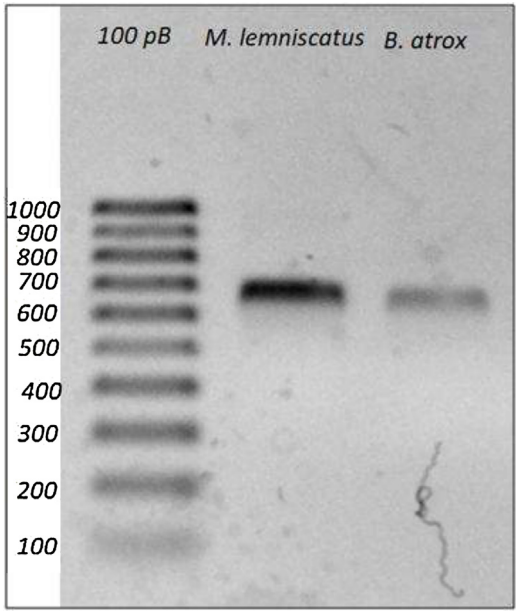

Fig. 1. Agarose gel (1%) electrophoresis of the PCR amplified from the snakes *M. lemniscatus* and *B. atrox* liver tissue cDNAs. PCR primers are described in Table 1. 100 bp, size markers.

The PLIγ models were submitted to molecular dynamic (MD) simulations using the program GROMACS (Groningen Machine for Chemical Simulation) v.5.0.5 [29,30] with GROMOS 96 54A7 force field [31]. The protein charged groups used were the correspondent of pH 7. The MD simulations were executed in the presence of explicit water molecules neutralized by addition of counter ions, in a periodic truncated cubic box, under constant temperature (298 K) and pressure (1.0 bar) held by coupling to an isotropic pressure and external heat bath [32,33]. In the cubic box, 5% of the water molecules were replaced by positive ions, Na^+, and negative ions, Cl^-, in equal amounts. The MD simulations were run with energy minimization using the steepest descent algorithm, followed by 2 ns of restrained protein position and by 100 ns of unrestrained protein position. The optimized PLI *in silico* models from *B. atrox* and from *M. lemniscatus* were further selected evaluating the stability in MD by average root mean square deviation (RMSD)/time graph of the protein backbone atoms and by overall stereochemical and energy quality in RAMPAGE [34] and ProSA-web [35], respectively.

The final models obtained after MD were analyzed in VMD [36]. The structural comparison were evaluated with RMSDs calculated using short fragment clustering by GESAMP (General Efficient Structural Alignment of Macromolecular Targets) approach [37]. Similar fold was evaluated by TM-Score generated by TM-align algorithm [38] and by PDBeFold [39]. The model residues accessible solvent area was calculated by AREAIMOL available in CCP4 suite [40]. The figures and surface illustrations were generated in CHIMERA [41] and Pymol (The PyMOL Molecular Graphics System, Version 1.3 Schrödinger, LLC.).

3. Results and discussion

Using oligonucleotides primers based on sequences of γ type phospholipase A_2 inhibitors from several families of snakes deposited at NCBI GenBank and RNA extracted from the liver tissue of specimens of the snakes *B. atrox* and *M. lemniscatus*, we obtained by RT-PCR fragments of approximately 600 base pairs (Fig. 1). These fragments were cloned in the vector *pGEM®-T Easy* (Promega Co, Madison, WI), resulting in 5 clones for *B. atrox* and 8 clones for *M. lemniscatus* (Fig. 2), from which nucleotide sequences were obtained.

Table 2
Comparative analysis of At.PLI1 and At.PLI2 sequences with the program *BLASTn*.

Identification	Species	Class	*Score*	Similarity	*Gaps*	*E-value*
EU155175	*B. moojeni*	γ	1057	98%	0%	0.0
EU155173	*B. jararacussu*	γ	1051	98%	0%	0.0
EU155166	*B. alternatus*	γ	1046	98%	0%	0.0
AY425346	*Lachesis muta muta*	γ	1046	98%	0%	0.0
EU155170	*B. jararaca*	γ	1018	97%	0%	0.0
CDU08289	*Crotalus d. terrificus*	γ	963	95%	0%	0.0
EU155168	*B. erythromelas*	γ	957	95%	2%	0.0
EU155177	*B. neuwiedi*	γ	946	95%	2%	0.0
AB018372	*Gloydiusb.siniticus*	γ	935	95%	0%	0.0
AB003472	*T. flavoviridis*	γ	857	93%	0%	0.0
AB559508	*P. elegans*	γ	852	93%	0%	0.0

*Data about the phospholipase A_2 inhibitors were selected by species, with a sequence of each being chosen for analysis. The program compared the sequences from this study with others deposited in GenBank.

Two consensus sequences were obtained from *B. atrox* and named At.PLI1 and At.PLI2 and two from *M. lemniscatus*, Mi.PLI1 and Mi.PLI2. We analyzed separately the sequences of each snake species as these are different at family level, Viperidae and Elapidae, respectively. By the sequence alignment, it was observed that the nucleotide sequences of At.PLI1 and 2 are similar to those from *B. moojeni* and *B. jararacussu* [42], *B. alternatus* [43], *Lachesis muta* [16], with 98% identity (Table 2). One sequence from each species with identity higher than 90% and an *E-value* of 0.0 was selected for analysis. The search data for homologous sequence segments (*Score*) show that the sequence of one PLIγ found in *B. moojeni* is the most similar to those obtained in this study (Table 2). Multiple nucleotide alignment confirmed the similarity between sequences. Deduced amino acid sequences were obtained using the program *ORF Finder*.

These data were used for a similarity search in the *GenBank* database and conserved domains were investigated using *BLASTp*. As shown in Fig. 3A, At.PLI1 and At.PLI2 amino acid sequences show homology to the PLIγs'three-finger fold, which are also present in urokinase-type plasminogen activator receptors (u-PAR) and in cell surface antigensfrom the superfamily Ly-6 and CD59 (Fig. 3). These results corroborate previous work with a PLA_2 inhibitor of *Naja naja kaouthia* [44]. Furthermore theoretical physico-chemical parameters of the *PLI* PLI of *B. atrox* (At.PLI1 and At.PLI2) were determined using *PROTParam* (isoelectric point and molecular mass) and compared to the same parameters of PLIγs of other snakes species. As shown in Table 3, close similarities exist between the *B. atrox* PLIs and the listed PLIγs.

The Mi.PLI1 and 2 sequences present divergence as to the inhibitor class in the search for similarity. Interestingly, the five sequences that presented the highest identities (89–91%) were inhibitors recorded in *Genbank* as PLIα and only two showed similarities with the γ-type (Table 4). The deduced translation of the nucleotide cracks was used for the multiple alignment and conserved domain search, according to the methodology described for *B. atrox*. Again, the similarity search resulted in PLI sequences of α and γ types (Table 5). Therefore, the PLIγ sequences of Brazilian snakes that presented the lowest identity (65–68%) were included in the analyses.

The search for conserved domains showed that Mi.PLI1 and Mi.PLI2 possess repeated cysteine residues in the three-finger fold (PLIγ) and not those of carbohydrate recognition (CRD) of Ca^{2+}-dependent lectins (CTLD family) characteristic of PLIα. Similar sequences recorded as PLIα were analyzed and also showed similarities with PLIγ domains.

Thus, At.PLI1 and 2, Mi.PLI1 and 2, as well as the crotoxin neutralizing factor (CNF), the most well-studied PLIγ isolated from *C. d.*

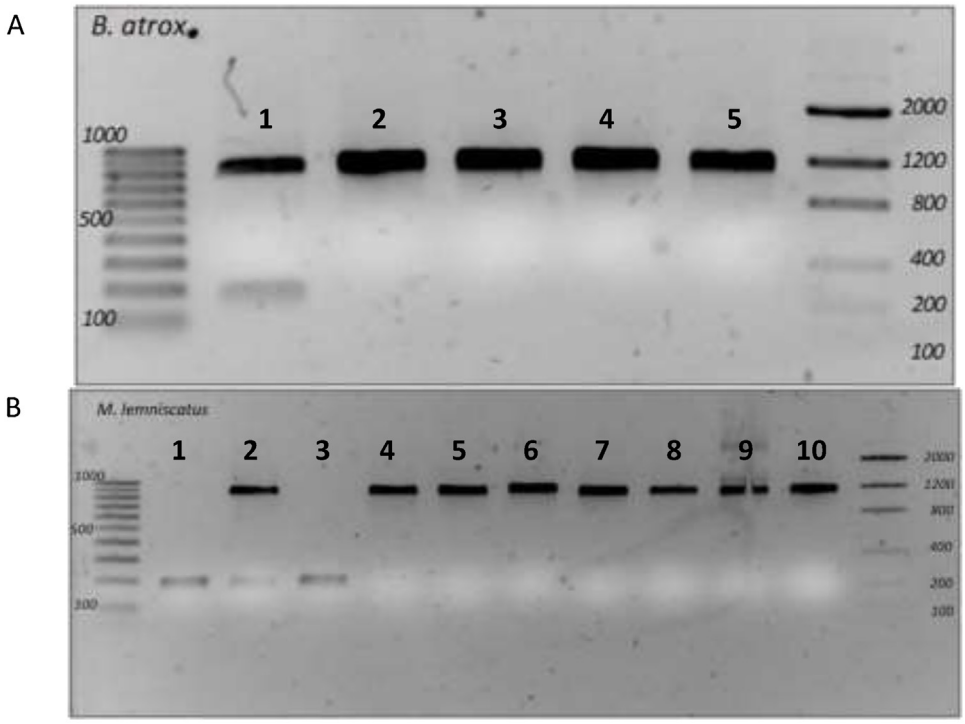

Fig. 2. Agarose gel (1%) of PLIγ cloned genes from *B. atrox* (bands 1–5 in A); and *M. lemniscatus* (in B). B) 2,4-10 bands correspond to amplified DNA fragments from selected colonies using the pGEM® -T Easy (Promega, Madison, WI, USA) primers T7 and SP6. 100 bp, size markers.

Table 3
Predicted/deducted biochemical characteristics of the phospholipase A_2 inhibitor from *B. atrox* compared with those of other snakes.

Inhibitor	Identification	sN° of Amino acids	Molecular mass (Da)	Isoelectric Point (pI)
At. PLI1	–	200	22196.2	5.97
At. PLI2	–	200	22180.2	5.97
B. moojeni	ABV91335.1	200	22181.1	5.97
B. jararacussu	ABV91332.1	200	22178.1	5.79
B. alternatus	ABV91326.1	200	22208.1	5.79
L. muta muta	P60592.1	200	22207.1	5.97
B. jararaca	ABV91331.1	200	22197.1	6.04
C. d. terrificus	Q90358.1	200	22267.4	6.07
B. erythromelas	ABV91328.1	200	22281.1	5.24
B. neuwiedi	ABV91336.1	200	22266.1	5.50

Table 4
Analysis of Mi.PLI1 and Mi.PLI2 sequences.

Identification	Species	Class	Identity	*Score*	*Gaps*	*E-value*
AF211165	*O. scutellatus*	α	91%	813	0%	0.0
AF211161	*Notechisater*	α	91%	808	0%	0.0
AJ249829	*Notechisscutatus*	α	90%	797	0%	0.0
AF211167	*O. microlepidotus*	α	90%	785	0%	0.0
AF211166	*P. textilis*	α	89%	769	0%	0.0
AB462512	*E. climacophora*	γ	89%	756	0%	0.0
AB021425	*E. quadrivirgata*	γ	88%	745	0%	0.0

terrificus, are orthologous to plasminogen activator factor from *H. sapiens*, characterized by three-finger domains [17], with e-values between e^{-26}/e^{-30} as calculated by HHPred server [45] (Table 6). In contrast, PLIαs are orthologous to lung surfactant protein D, which presents a carbohydrate recognition domain [43,46]. Interestingly, these sequences from Elapidae snakes previously deposited as PLIαs in NCBI (GIs: 6685092, 6685094, 5931772, 6685090) present similar e-values to plasminogen activator factor suggesting that these sequences are in fact PLIγs. Furthermore, these Elapidae sequences show an E-value around e-39 for the plasminogen activator factor domain observed in CNF, as seen in PFAM software [47].

Phylogenetic tree using these sequences from Elapidae, At.PLI1 and At.PLI2, Mi.PLI1 and 2 and all other PLIγs available on NCBI databank shows that Elapidae sequences nest in a clade with PLIγs from non-venomous Colubridae snakes (Fig. 3B). Interestingly, sequences from venomous Viperidae family also nest in a clade with sequences from snakes from a non-venomous family (Phytonidae) (Fig. 3B). Amino acid sequences alignment of these sequences shows well conserved regions in all PLIγs (Fig. 3A).

The similarities of the transcripts to GenBank were verified in the multiple alignment, and conserved domain regions were identified. It was observed that there is similarity between the recorded sequences, such as PLIαs and PLIγs. Moreover, it is noted that Elapidae sequences possess well-conserved regions different from those of *Bothrops*. In some of these places, Mi.PLI sequences are similar only to *Micrurus*, and in others to *Bothrops* (Fig. 3). Finally, a sequence of the *B. jararacussu* CTLD chosen randomly from *Genbank* was aligned to Mi.PLI and there was no similarity. The sequences that are recorded in *Genbank* as PLIαs (Table 5) may possibly be those referred to as Elapidae PLIγs in Table 3, since there are no publications of PLIαs in these species yet. The studies about PLIγ in Table 5 were published [40,46].

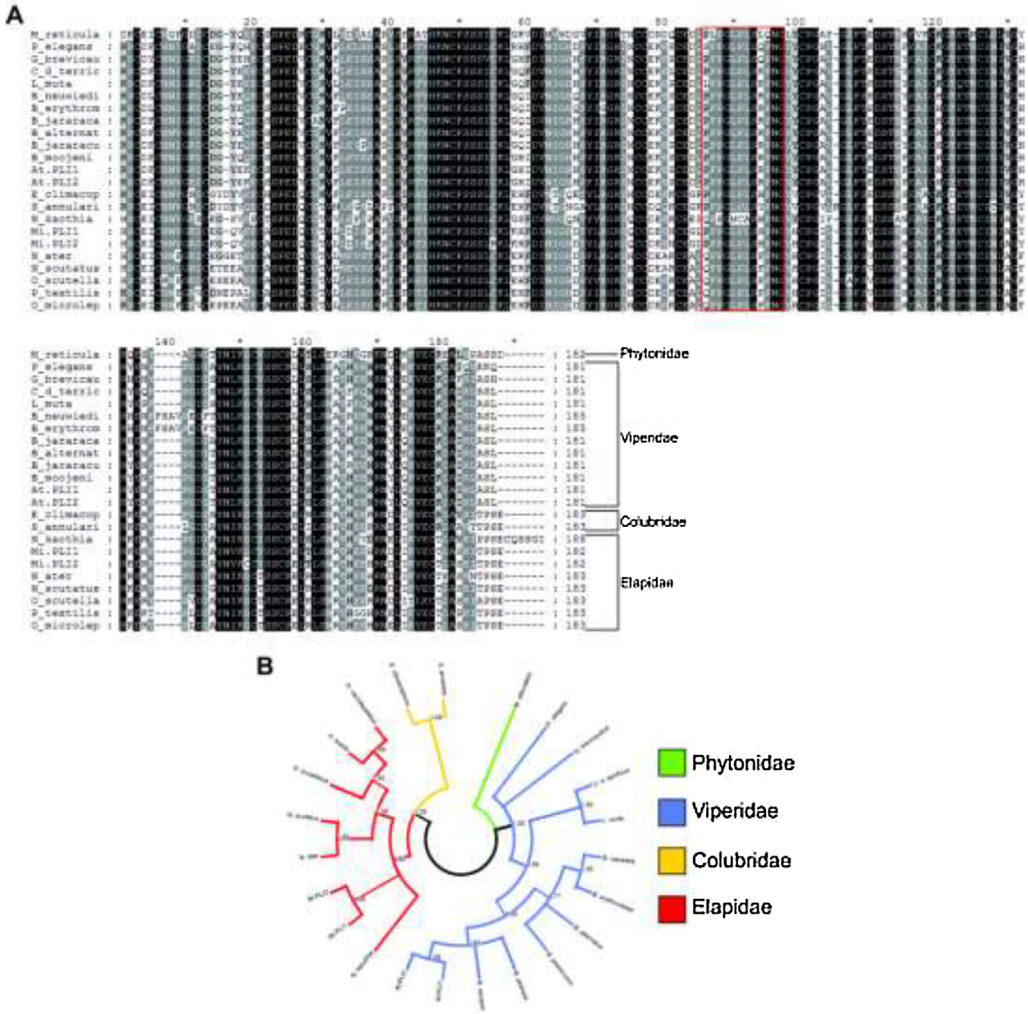

Fig. 3. Amino acid sequences alignment (A) and phylogenetic analyses (B) of gamma phospholipases A_2 inhibitors (PLIγs) of snakes from different families. A) The decapeptide (87–96) is highlighted in the red box. B) Phlylogenetic tree resulted from the aligned sequences. Each branch color corresponds to a different snake family. PLIγs sequences used for the alignment were: *Malayopython reticulates* (GI: 8163992); *Protobothrops elegans* (302698904); *Gloydius brevicaudus siniticus* (26454644); *Crotalus* neutralization factor from *Crotalus durissus terrificus* (45477157); *Lachesis muta muta* (45477023); *Bothrops neuwiedi* (157885078); *Bothrops erythromelas* (157885064); *Bothrops jararaca* (157885068); *Bothrops alternates* (157885058); *Bothrops jararacussu* (157885072); *Bothrops moojeni* (157885076); At.PLI1 (this work); At.PLI2 (this work); *Elaphe climacophora* (226235139); *Sinonatrix annularis* (385843188); *Naja kaouthia* (47117137); Mi.PLI1 (this work); Mi.PLI12 (this work); *Notechis ater*(6685090); *Notechis scutatus* (5931772); *Oxyuranus scutellatus* (6685092); *Pseudonaja textilis* (6685096) and *Oxyuranus microlepidotus* (6685094). (For interpretation of the references to colour in this figure legend, the reader is referred to the web version of this article.)

PLIs were modeled using domains 2 and 3 of mammalian uPARs templates and were submitted to 100 ns classical MD. Models were stabilized within the first 20 ns with a RMSD of 5 Å. At.PLI2 (m.At.PLI2) and Mi.PLI1 (m.Mi.PLI1) models have 94.4% and 92.2% of residues in favored and allowed regions and Z-score of −4.48 and −5.08, respectively, whose values are within expected crystallographic structures of similar protein size.

M.At.PLI2 and m.i.PLI1 kept initial fold after molecular dynamics stabilization as shown by a low RMSD deviation of approximately 6 Å. This fold is also seen in uPAR as confirmed by T-scores above 0.6 when *in silico* models are compared to the uPARs modeling templates (Fig. 4A_1, B_1 and C). This feature is confirmed when comparing the studied models to all available structures in the protein databank by PDBeFold, where uPARs are top in the list with Z-scores between 4 and 5. As a matter of fact, uPAR is an extracellular protein containing 283 residues divided into three domains (approximate 90 residues each) that adopt a three-finger fold and that are classified as Ly-6/uPAR/α-neurotoxin protein domain family [27,28]. M.At.PLI2 and m.Mi.PLI1 homology to uPAR confirms them as PLIγs, as these inhibitors are composed of two structural units of highly conserved tandem repeats of half cysteines known as three-finger motifs.

M.At.PLI2 and m.Mi.PLI1 comparison confirms conservation of the fold with some local differences already expected for proteins from different snake families (Fig. 4A_2 and B_2), with a superposition RMSD of 2.3 Å (75% of matching residues) and T-score of 0.54. β-sheets and disulphide bridges (yellow sticks in Fig. 4A_2 and B_2) are the most similar regions in the studied PLIs (coloured in blue in Fig. 4A_2 and B_2); on the other hand, extremities of β-sheets, loops and in more exposed regions of models were coloured whiter as they deviates more than bluish regions. Few regions coloured in red were excluded by superimposition algorithm since that they present high structural deviation. Despite of the few structural studies on snake PLIs structures available, CNF is one of the most studied PLIγ and its *in silico* structure has been modelled [17]. The superposition of m.At.PLI2 and m.Mi.PLI1 with the *in silico* model of CNF [17] generated RMSD of 2.7 and 2.9 Å from matching 85 and 73% of residues, respectively (Fig. 4D). PLIγ were described as possessing high-order quaternary structure, such as trimers [49] or tetramers [17], and m.At.PLIs and m.Mi.PLIs have similar tertiary

Table 5
Similarity of the sequences used to analyze the *M. lemniscatus* inhibitor.

Class	Family	Species	Identification	Maximum Identity (%)	Reference
A	Elapidae	*Notechis ater*	AAF23778	85	[54]
		Oxyuranus scutellatus	AAF23781	83	[54]
		Pseudonaja textilis	AAF23783	82	[54]
		Notechis scutatus	CAB56617	82	[8]
		Oxyuranus microlepidotus	AAF23785	81	[54]
Γ	Elapidae	*Elaphe climacophora*	BAH47550	82	[48]
	Viperidae	*B. moojeni*	ABV91335	68	[42]
		B. jararaca	ABV91331	68	[42]
		B. alternatus	ABV91326	68	[42]
		B. jararacussu	ABV91333	67	[42]
		B. neuwiedi	ABV91336	66	[42]
		B. erythromelas	ABV91328	65	[42]

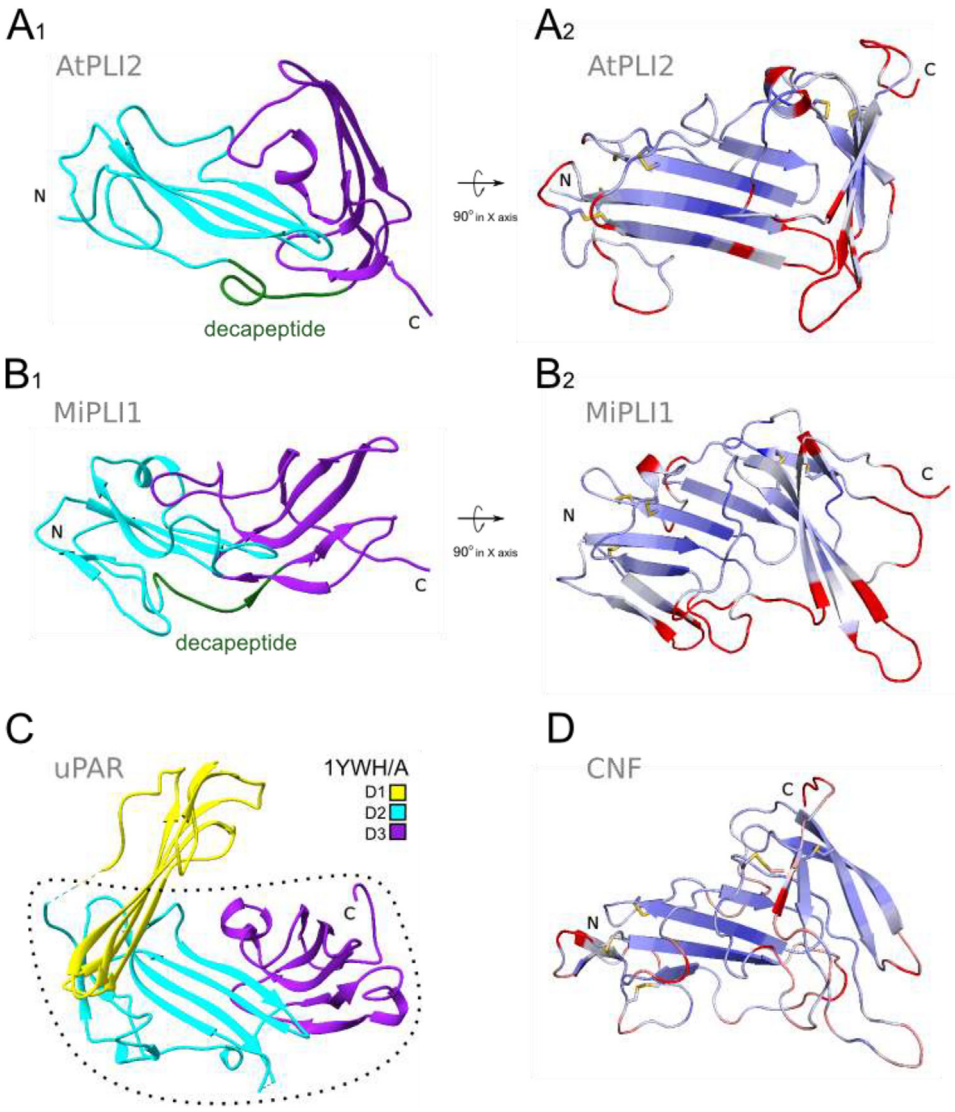

Fig. 4. Fold similarities between *in silico* models of AtPLI2 and MiPLI1 and the crystallographic structure of a human Urokinase plasminogen activator surface receptor (uPAR). Structures in cartoon representation of A_1-A_2 *Bothrops atrox* PLI (AtPL2), B_1-B_2 *M. lemniscatus* PLI (MiPLI1), C) *Homo sapiens* uPAR (1YWH/chainA) and D) *C. d. terrificus* CNF. They were orientated after superimposition of four long β-sheets colored in cyan. Molecules in A_1, B_1 and C are in a 90° rotation in the horizontal axis in relationship to A_2, B_2 and D. Molecules in A_1, B_1 and C were generated in Chimera and were colored according to *Homo sapiens* uPAR domains: D1 (yellow), D2 (cyan) and D3 (purple); moreover the PLI decapeptide, the putative PLA_2s interaction site, is colored in green and is correspondent to the end of uPAR D2. Molecules in A_2, B_2 and D were generated in Pymol and were colored based on distance generated by superimposition in a range of 2.5 Å in white to 0 Å in blue, whereas the red are residues excluded in superimposition. While the distances in AtPLI2 in A_2 and MiPLI1 in B_2 were calculated using only these two models, CNF distances in D were calculated by the mean of the distances with both previous models. The *in silico* PLI models shares conservancy of β-sheets (bluish) and disulfide bridges (yellow sticks in A_2, B_2, and D). (For interpretation of the references to colour in this figure legend, the reader is referred to the web version of this article.)

Table 6
Structural homology evaluation of gamma phospholipases A_2 inhibitors sequences in comparison with crystal structure of human urokinase plasminogen activator.

Crystal Structure of Urokinase Plasminogen Activator from *H. sapiens* (Chain U; PDB ID 2FD6)		
	Score	E-value
At.PLI2	187.17	4.3 e-26
Mi.PLI1	184.85	4.4e-26
CNF	212.63	1.3e-30
O. scutellatus PLI*	187.21	2.5e-26
O. microlepidotus PLI*	188.38	1.6e-26
N. scutatus PLI*	189.51	5.8e-27
N. ater PLI*	192.5	1.8e-27
P. textilis PLI*	187.72	1.4e-26

Score and e-values were obtained by HHPred software [45]. The sequences marked with * were previously noted as alpha phospholipases A_2 inhibitors. At.PLI2 and Mi.PLI1 were described in this work. CNF is *Crotalus* neutralization factor, a γ PLI from *Crotalus durissus terrificus* (GI: 45477157). The PLIs from *Oxyuranus scutellatus*, *Oxyuranus microlepidotus*, *Nothechis scutatus*, *Notechis ater* and *Pseudonaja textilis* were found on NCBI database with the following GI codes: 6685092, 6685094, 5931772, 6685090.

structures to CNF. Therefore, this probably indicates the studied proteins arrange in higher quaternary structure. The structural similarities and differences in studied PLIs models are also seen in CNF *in silico* model (Fig. 4D).

Snake PLA_2s and PLI share a high variability in sequences, which, in the case of the inhibitors, could be important to efficiently neutralize different PLA_2. Although, a specific region from residue 107–116 is conserved among different PLIγs (Fig. 3 in red box, different numbering is due to the absence of signal peptide in alignment). The synthetic decapeptide, called P-PB.III, based on the non venomous snake *Python reticulatus* PLIγ sequence (^{107}PGLPLSLQNG^{116}) was shown to recognize different PLA_2s and inhibit their catalytic activity [50]. Similarly to P-PB.III, At.PLI and Mi.PLI sequences possess the decapeptides ^{107}PGLPLSRPNG^{116} and ^{107}PGLPLSHPNG^{116}, respectively, which differs only by two substitutions, in the positions 112 and 113. This decapeptide in m.At.PLI2 and m.Mi.PLI1 are exposed to the solvent for both proteins with no secondary structure (Fig. 4A_1 and B_1 in green), with exception of the last three residues in m.Mi.PLI1 which presents β-sheet conformation. The sum of accessible solvent area for this decapeptide in At.PLI1 and Mi.PLI1 model are approximately 620 and 680 Å^2, respectively. Despite similar exposed areas and sequence conservation, the different decapeptides possess different conformations, as its RMSD of m.At.PLI2 and m.Mi.PLI1 is 3.9 Å. Comparing to CNF decapeptide, m.At.PLI2 shares more similarities than m.Mi.PLI1, as their RMSD is 2.7 and 3.6 Å, respectively. The PLIγ broad inhibiting spectrum by different snake venom PLA_2s [50–53] may be related to the conservation of decapeptide sequence together with its solvent exposition and loop flexibility. Thus, such observations strength the hypothesis that the decapeptide (107–116) may participate in PLA_2s interaction and eventual inhibition.

4. Conclusion

The methodology applied to the amplification of the liver tissue genetic material from the snakes *B. atrox* and *M. lemniscatus* showed to be efficient in identifying the phospholipase A_2 inhibitor transcripts.

The presence of γ class inhibitors was proven for the species *B. atrox*, which presented elevated similarity to other sequences characterized as such. The sequences from *M. lemniscatus* presented particular characteristics of similarity with other elapid or bothropic snakes at preserved sites. However, the presence of a three-finger fold specific to the PLIγ group and the absence of a CRD domain specific to PLIαs in the *in silico* models, among their similar tertiary structure to CNF, suggest that the studied inhibitors are PLIγ. The conservation of the primary structure of decapeptide among different PLIs, which was hypothesized to be the responsible region for PLA_2s inhibition, is not followed by conservation of tertiary structure seen in the *in silico* evaluated models and this high deviation may be related to the PLIγ broad inhibiting spectrum of different snake venom PLA_2s.

Conflict of interest

There are no conflicts of interest.

Acknowledgements

The authors acknowledge Conselho Nacional de Desenvolvimento Científico e Tecnológico (CNPq), Coordenação de Aperfeiçoamento de Pessoal de Nível Superior (CAPES), Instituto Nacional de Ciência e Tecnologia em Pesquisa Translacional em Saúde e Ambiente na Região Amazônica (INCT-INPeTAm), Instituto Nacional de Ciência e Tecnologia em Toxinas (INCT-Tox), Fundação de Amparo à Pesquisa do Estado de Rondônia (FAPERO), and Fundação de Amparo à Pesquisa do Estado de São Paulo for financial support. RJB and CAHF acknowledge their grants from Fundação de Amparo à Pesquisa do Estado de São Paulo (FAPESP). The authors thank the Program for Technological Development in Tools for Health-PDTIS-FIOCRUZ for use of its facilities. Amy Grabner provided the English editing of the manuscript.

References

[1] J.M. Gutiérrez, B. Lomonte, G. León, A. Alape-Girón, M. Flores-Díaz, L. Sanz, et al., Snake venomics and antivenomics: proteomic tools in the design and control of antivenoms for the treatment of snakebite envenoming, J. Proteomics 72 (2009) 165–182.
[2] N.R. Casewell, G.a. Huttley, W. Wüster, Dynamic evolution of venom proteins in squamate reptiles, Nature 3 (2012) 1066.
[3] B. Lomonte, J.M. Gutiérrez, Phospholipases A2 from viperidae snake venoms: how do they induce skeletal muscle damage? Acta Chim. Slov. 58 (2011) 647–659.
[4] E.A. Dennis, J. Cao, Y.-H. Hsu, V. Magrioti, G. Kokotos, Phospholipase A2 enzymes: physical structure, biological function, disease implication, chemical inhibition, and therapeutic intervention, Chem. Rev. 111 (2011) 6130–6185, http://dx.doi.org/10.1021/cr200085w.
[5] R.P. Samy, P. Gopalakrishnakone, V.T.K. Chow, Therapeutic application of natural inhibitors agaisnt snake venom phospholipase A_2, Bioinformation 8 (2012).
[6] J.E. Biardi, C.Y.L. Ho, J. Marcinczyk, K.P. Nambiar, Isolation and identification of a snake venom metalloproteinase inhibitor from California ground squirrel (Spermophilus beecheyi) blood sera, Toxicon 58 (2011) 486–493.
[7] S. Marcussi, C.D. Sant'Ana, C.Z. Oliveira, A.Q. Rueda, D.L. Menaldo, R.O. Beleboni, et al., Snake venom phospholipase A2 inhibitors: medicinal chemistry and therapeutic potential, Curr. Top. Med. Chem. 7 (2007) 743–756.
[8] P.G. Hains, B. Nield, S. Sekuloski, R. Dunn, K. Broady, Sequencing and two-dimensional structure prediction of a phospholipase A2 inhibitor from the serum of the common tiger snake (Notechis scutatus), J. Mol. Biol. 312 (2001) 875–884.
[9] K. Okumura, S. Inoue, K. Ikeda, K. Hayashi, cDNA cloning and bacterial expression of phospholipase A2 inhibitor PLI from the serum of the Chinese mamushi, Agkistrodon blomhoffii siniticus, Biochim. Biophys. Acta 1441 (1999) 51–60.
[10] S. Lizano, Y. Angulo, B. Lomonte, J.W. Fox, G. Lambeau, M. Lazdunski, et al., Two phospholipase A2 inhibitors from the plasma of Cerrophidion (Bothrops) godmani which selectively inhibit two different group-II phospholipase A2 myotoxins from its own venom: isolation, molecular cloning and biological properties, Biochem. J. 639 (2000) 631–639.
[11] S. Donnini, F. Finetti, S. Francese, F. Boscaro, F.R. Dani, F. Maset, et al., A novel protein from the serum of Python sebae, structurally homologous with type-γ phospholipase A2 inhibitor, displays antitumour activity, Biochem. J. 440 (2011) 251–262, http://dx.doi.org/10.1042/BJ20100739.
[12] M.I. Estevão-Costa, C.A.H. Fernandes, M. de A. Mudadu, G.R. Franco, M.R.M. Fontes, C.L. Fortes-Dias, Structural and evolutionary insights into endogenous alpha-phospholipase A2 inhibitors of Latin American pit vipers, Toxicon 112 (2016) 35–44, http://dx.doi.org/10.1016/j.toxicon.2016.01.058.
[13] S. Lizano, G. Domont, J. Perales, Natural phospholipase A2 myotoxin inhibitor proteins from snakes, mammals and plants, Toxicon 42 (2003) 963–977, http://dx.doi.org/10.1016/j.toxicon.2003.11.007.

[14] K. Okumura, S. Inoue, K. Ikeda, K. Hayashi, Identification of b-type phospholipase A2 inhibitor in a nonvenomous snake, Elaphe quadrivirgata, Arch. Biochem. Biophys. 408 (2002) 124–130.
[15] C.L. Fortes-Dias, Endogenous inhibitors of snake venom phospholipases A2 in the blood plasma of snakes, Toxicon 40 (2002) 481–484, http://dx.doi.org/10.1016/S0041-0101(01)00274-4.
[16] C.L. Fortes-Dias, C.J. Barcellos, M.I. Estevão-Costa, Molecular cloning of a g-phospholipase A2 inhibitor from Lachesis muta muta (the bushmaster snake), Toxicon 41 (2003) 909–917, http://dx.doi.org/10.1016/S0041-0101(03)00073-4.
[17] C.L. Fortes-Dias, P.L. Ortolani, C.A.H. Fernandes, K.R. Lobo, L. Amaral de Melo, M.H. Borges, et al., Insights on the structure of native CNF, an endogenous phospholipase A2 inhibitor from Crotalus durissus terrificus, the South American rattlesnake, Biochim. Biophys. Acta 2014 (1844) 1569–1579, http://dx.doi.org/10.1016/j.bbapap.2014.05.001.
[18] Z. Le, X. Li, P. Yuan, P. Liu, C. Huang, Orthogonal optimization of prokaryotic expression of a natural snake venom phospholipase A2 inhibitor from Sinonatrix annularis, Toxicon 108 (2015) 264–271, http://dx.doi.org/10.1016/j.toxicon.2015.10.018.
[19] B.S. Cummings, J. Mchowat, R.G. Schnellmann, Phospholipase A2s in cell injury and death, J. Pharmacol. Exp. Ther. 294 (2000) 793–799.
[20] M.-M. Thwin, R.P. Samy, S.D. Satyanarayanajois, P. Gopalakrishnakone, Venom neutralization by purified bioactive molecules: synthetic peptide derivatives of the endogenous PLA(2) inhibitory protein PIP (a mini-review), Toxicon 56 (2010) 1275–1283, http://dx.doi.org/10.1016/j.toxicon.2009.12.023.
[21] R.P. Samy, M.M. Thwin, B.G. Stiles, H. Bow, V.T.K. Chow, P. Gopalakrishnakone, Therapeutic potential of peptides with neutralizing ability towards the venom and toxin (CaTx-I) of crotalus adamanteus, Curr. Top. Med. Chem. 11 (2011) 2540–2555 (Accessed June 17 2016) http://www.ncbi.nlm.nih.gov/pubmed/21682682.
[22] S.F. Altschul, W. Gish, W. Miller, E.W. Myers, D.J. Lipman, Basic local alignment search tool, J. Mol. Biol. 215 (1990) 403–410, http://dx.doi.org/10.1016/S0022-2836(05)80360-2.
[23] R.C. Edgar, MUSCLE: multiple sequence alignment with high accuracy and high throughput, Nucleic Acids Res. 32 (2004) 1792–1797, http://dx.doi.org/10.1093/nar/gkh340.
[24] F. Ronquist, J.P. Huelsenbeck, MrBayes 3: Bayesian phylogenetic inference under mixed models, Bioinformatics 19 (2003) 1572–1574.
[25] D.R. Madison, W.P. Madison, Mesquite: A Modular System For Evolutionary Analysis, 2015.
[26] L.A. Kelley, S. Mezulis, C.M. Yates, M.N. Wass, M.J.E. Sternberg, The Phyre2 web portal for protein modeling, prediction and analysis, Nat. Protoc. 10 (2015) 845–858, http://dx.doi.org/10.1038/nprot.2015.053.
[27] L. Lin, H. Gårdsvoll, Q. Huai, M. Huang, M. Ploug, Structure-based engineering of species selectivity in the interaction between urokinase and its receptor: implication for preclinical cancer therapy, J. Biol. Chem. 285 (2010) 10982–10992, http://dx.doi.org/10.1074/jbc.M109.093492.
[28] P. Llinas, M.H. Le Du, H. Gårdsvoll, K. Danø, M. Ploug, B. Gilquin, et al., Crystal structure of the human urokinase plasminogen activator receptor bound to an antagonist peptide, EMBO J. 24 (2005) 1655–1663, http://dx.doi.org/10.1038/sj.emboj.7600635.
[29] H.J.C. Berendsen, D. van der Spoel, R. van Drunen, GROMACS: A message-passing parallel molecular dynamics implementation, Comp. Phys. Commun. 91 (1995) 43–56.
[30] B. Hess, C. Kutzner, D. van der Spoel, E. Lindahl, GROMACS 4: algorithms for highly efficient, load-balanced, and scalable molecular simulation, J. Chem. Theory Comput. 4 (2008) 435–447, http://dx.doi.org/10.1021/ct700301q.
[31] N. Schmid, A.P. Eichenberger, A. Choutko, S. Riniker, M. Winger, A.E. Mark, et al., Definition and testing of the GROMOS force-field versions 54A7 and 54B7, Eur. Biophys. J. 40 (2011) 843–856, http://dx.doi.org/10.1007/s00249-011-0700-9.
[32] H.J.C. Berendsen, J.P.M. Postma, W.F. van Gunsteren, J. Hermans, Interaction Models for Water in Relation to Protein Hydration, in: B. Pullman (Ed.), Reidel, Dordr., 1981, pp. 331–342 (Intermol. Forces).
[33] H.J.C. Berendsen, J.P.M. Postma, W.F. van Gunsteren, A. DiNola, J.R. Haak, Molecular dynamics with coupling to an external bath, J. Chem. Phys. 81 (1984) 3684–3690, http://dx.doi.org/10.1063/1.448118.
[34] S.C. Lovell, I.W. Davis, W.B. Arendall, P.I.W. de Bakker, J.M. Word, M.G. Prisant, et al., Structure validation by Calpha geometry: phi, psi and Cbeta deviation, Proteins 50 (2003) 437–450, http://dx.doi.org/10.1002/prot.10286.
[35] M. Wiederstein, M.J. Sippl, ProSA-web: interactive web service for the recognition of errors in three-dimensional structures of proteins, Nucleic Acids Res. 35 (2007) 3.
[36] W. Humphrey, A. Dalke, K. Schulten, VMD: visual molecular dynamics, J. Mol. Graph. 14 (33–38) (1996) 27–28.
[37] E. Krissinel, Enhanced fold recognition using efficient short chain fragment clustering, J. Mol. Biochem. 1 (2012) 76–85.
[38] Y. Zhang, J. Skolnick, TM-align: a protein structure alignment algorithm based on the TM-score, Nucleic Acids Res. 33 (2005) 2302–2309, http://dx.doi.org/10.1093/nar/gki524.
[39] E. Krissinel, K. Henrick, Secondary-structure matching (SSM), a new tool for fast protein structure alignment in three dimensions, Acta Crystallogr. D Biol. Crystallogr. 60 (2004) 2256–2268, http://dx.doi.org/10.1107/S0907444904026460.
[40] M.D. Winn, C.C. Ballard, K.D. Cowtan, E.J. Dodson, P. Emsley, P.R. Evans, et al., Overview of the CCP4 suite and current developments, Acta Crystallogr. Sect. D Biol. Crystallogr. 67 (2011) 235–242, http://dx.doi.org/10.1107/S0907444910045749.
[41] E.F. Pettersen, T.D. Goddard, C.C. Huang, G.S. Couch, D.M. Greenblatt, E.C. Meng, et al., UCSF Chimera-a visualization system for exploratory research and analysis, J. Comput. Chem. 25 (2004) 1605–1612, http://dx.doi.org/10.1002/jcc.20084.
[42] M.I. Estevão-Costa, B.C. Rocha, M. de Alvarenga Mudado, R. Redondo, G.R. Franco, C.L. Fortes-Dias, Relationships of endogenous g-phospholipase A2 inhibitors in brazilian bothrops snakes (Viperidae, crotalinae), Toxicon 52 (2008) 122–129, http://dx.doi.org/10.1016/j.toxicon.2008.04.167.
[43] N. a Santos-Filho, C. a H. Fernandes, D.L. Menaldo, A.J. Magro, C.L. Fortes-Dias, M.I. Estevão-Costa, et al., Molecular cloning and biochemical characterization of a myotoxin inhibitor from Bothrops alternatus snake plasma, Biochimie 93 (2011) 583–592, http://dx.doi.org/10.1016/j.biochi.2010.11.016.
[44] K. Hayashi, N. Ohkura, S. Inoue, K. Ikeda, Isolation and characterization of a phospholipase A2 inhibitor from the blood plasma of the Thailand cobra Naja naja kaouthia, Biochem. Biophys. Res. Commun. 200 (1994) 784–788.
[45] J. Söding, A. Biegert, A.N. Lupas, The HHpred interactive server for protein homology detection and structure prediction, Nucleic Acids Res. 33 (2005) 244–248, http://dx.doi.org/10.1093/nar/gki408.
[46] K. Okumura, A. Ohno, M. Nishida, K. Hayashi, K. Ikeda, S. Inoue, Mapping the region of the??-type phospholipase A2 inhibitor responsible for its inhibitory activity, J. Biol. Chem. 280 (2005) 37651–37659, http://dx.doi.org/10.1074/jbc.M507250200.
[47] R.D. Finn, P. Coggill, R.Y. Eberhardt, S.R. Eddy, J. Mistry, A.L. Mitchell, et al., The Pfam protein families database: towards a more sustainable future, Nucleic Acids Res. 44 (2015), http://dx.doi.org/10.1093/nar/gkv1344.
[48] R. Shirai, M. Toriba, K. Hayashi, K. Ikeda, S. Inoue, Identification and characterization of phospholipase A2 inhibitors from the serum of the Japanese rat snake, Elaphe climacophora, Toxicon 53 (2009) 685–692, http://dx.doi.org/10.1016/j.toxicon.2009.02.001.
[49] N. Ohkura, Y. Kitahara, S. Inoue, K. Ikeda, K. Hayashi, Isolation and amino acid sequence of a phospholipase A2 inhibitor from the blood plasma of the sea krait, Laticauda semifasciata, J. Biochem. 125 (1999) 375–382.
[50] M.-M. Thwin, R.L. Satish, S.T.F. Chan, P. Gopalakrishnakone, Functional site of endogenous phospholipase A2 inhibitor from python serum, Eur. J. Biochem. 269 (2002) 719–727.
[51] C.L. Fortes-Dias, M.L. Jannotti, F.J. Franco, A. Magalhães, C.R. Diniz, Studies on the specificity of CNF, a phospholipase A2 inhibitor isolated from the blood plasma of the South American rattlesnake (Crotalus durissus terrificus). I. Interaction with PLA2 from Lachesis muta muta snake venom, Toxicon Off. J. Int. Soc. Toxinol. 37 (1999) 1747–1759.
[52] S. Inoue, A. Shimada, N. Ohkura, K. Ikeda, Y. Samejima, T. Omori-Satoh, et al., Specificity of two types of phospholipase A2 inhibitors from the plasma of venomous snakes, Biochem. Mol. Biol. Int. 41 (1997) 529–537.
[53] C.Z. Oliveira, N.A. Santos-Filho, D.L. Menaldo, J. Boldrini-Franca, J.R. Giglio, L.A. Calderon, et al., Structural and functional characterization of a γ-type phospholipase A2 inhibitor from bothrops jararacussu snake plasma, Curr. Top. Med. Chem. 11 (2011) 2509–2519.
[54] K.W. Sekuloski, S. Dunn, R.D. Broady, Identification of Alpha and Beta Subunit Isoforms of a Phospholipase A2 Inhibitor Isolated from Four Species of Elapidae, University of Technology, Sydney, 2000.